4184–4191 *Nucleic Acids Research, 2003, Vol. 31, No. 14*
DOI: 10.1093/nar/gkg475

Mycobacterium tuberculosis RecA intein, a LAGLIDADG homing endonuclease, displays Mn^{2+} and DNA-dependent ATPase activity

N. Guhan and K. Muniyappa*

Department of Biochemistry, Indian Institute of Science, Bangalore 560 012, India

Received February 26, 2003; Revised April 28, 2003; Accepted May 23, 2003

ABSTRACT

***Mycobacterium tuberculosis* RecA intein (PI-MtuI), a LAGLIDADG homing endonuclease, displays dual target specificity in response to alternative cofactors. While both ATP and Mn^{2+} were required for optimal cleavage of an inteinless *recA* allele (hereafter referred to as cognate DNA), Mg^{2+} alone was sufficient for cleavage of ectopic DNA sites. In this study, we have explored the ability of PI-MtuI to catalyze ATP hydrolysis in the presence of alternative metal ion cofactors and DNA substrates. Our results indicate that PI-MtuI displays maximum ATPase activity in the presence of cognate but not ectopic DNA. Kinetic analysis revealed that Mn^{2+} was able to stimulate PI-MtuI catalyzed ATP hydrolysis, whereas Mg^{2+} failed to do so. Using UV cross-linking, limited proteolysis and amino acid sequence analysis, we show that ^{32}P-labeled ATP was bound to a 14 kDa peptide containing the putative Walker A motif. Furthermore, the limited proteolysis approach disclosed that cognate DNA was able to induce structural changes in PI-MtuI. Mutation of the presumptive metal ion-binding ligands (Asp122 and Asp222) in the LAGLIDADG motifs of PI-MtuI impaired its affinity for ATP, thus resulting in a reduction in or loss of its endonuclease activity. Together, these results suggest that PI-MtuI is a (cognate) DNA- and Mn^{2+}-dependent ATPase, unique from the LAGLIDADG family of homing endonucleases, and implies a possible role for ATP hydrolysis in the recognition and/or cleavage of homing site DNA sequence.**

INTRODUCTION

Inteins are enzymes encoded by intervening sequences embedded in-frame within protein-coding genes. Most of these enzymes possess both protein splicing and homing endonuclease activities. The latter activity has been implicated in the lateral transfer of intervening sequences via a process termed 'homing', leading to the rearrangement of organelle as well as nuclear genomes (1–6). One hallmark of homing endonucleases is their ability to recognize and cleave extended (14–40 bp) but degenerate sequences that are normally centered in inteinless alleles (1,7). Traditionally, homing endonucleases are grouped based on their conserved sequence motifs into LAGLIDADG, GIY-YIG, His-Cys box and H-N-H families (1,5,6,8). Among these, the LAGLIDADG family is the largest, most widespread and most studied class of homing endonucleases. Several lines of evidence have indicated that homing endonucleases with one LAGLIDADG motif act as homodimers, whereas enzymes bearing two such motifs in the same polypeptide act as monomers (9–12). In all cases, LAGLIDADG enzymes display extreme specificity for their recognition sequences, and Mg^{2+} is the preferred cofactor for cleavage of inteinless alleles.

However, *Mycobacterium tuberculosis* RecA intein (PI-MtuI), a member of the LAGLIDADG family of homing endonucleases, displays two key functional differences. First, PI-MtuI exhibits dual target specificity in response to alternative cofactors (13,14). Second, while both ATP and Mn^{2+} are required for cleavage of the inteinless *recA* allele (hereafter referred to as cognate DNA), Mg^{2+} alone was sufficient for cleavage of ectopic DNA sites (13,14). These observations raised the possibility of whether PI-MtuI can bind ATP and catalyze its hydrolysis. ATP hydrolysis by PI-MtuI may be necessary for its turnover, for DNA translocase activity or cleavage of cognate DNA sequence.

In this study, we have investigated the basis of ATP-dependent cleavage of cognate DNA by PI-MtuI. We observed that PI-MtuI was able to bind ATP with high affinity and catalyze its hydrolysis. Importantly, this activity was substantially higher in the presence of Mn^{2+} and cognate DNA compared to ectopic DNA or Mg^{2+}. Consistent with this observation, cognate DNA was able to induce conformational changes in the native structure of PI-MtuI. Although the catalytic mechanisms underlying the cleavage of DNA by homing endonucleases are beginning to be understood, our results provide new insights into the role of ATP hydrolysis in the cleavage of cognate DNA.

MATERIALS AND METHODS

Reagents and DNA

All the chemicals used in this study were of analytical grade. The buffers were prepared using deionized water. ATP was

*To whom correspondence should be addressed. Tel: +91 80 360 0278; Fax: +91 80 360 0814; Email: kmbc@biochem.iisc.ernet.in

purchased from Amersham Biosciences Inc. Asia Pacific Ltd (Hong Kong). It was dissolved in water, the pH was adjusted to 7 with NaOH, and its concentration was estimated spectrophotometrically using an extinction coefficient of ε_{259} = 15 400/M/cm. [γ-^{32}P]ATP (6000 Ci/mmol) and [α-^{32}P]ATP (3000 Ci/mmol) were purchased from Perkin-Elmer Life Sciences. PEI–cellulose thin layer chromatography (TLC) sheets were purchased from Merck. Negatively supercoiled pEJ244 and bacteriophage M13 DNAs were prepared by sucrose density gradient centrifugation (15). The fractions containing DNA were pooled and precipitated with ethanol. DNA was collected by centrifugation, the pellet was resuspended in 10 mM Tris–HCl buffer (pH 7.5) containing 1 mM EDTA and dialyzed against the same buffer for 6 h. The nature of negatively supercoiled DNA was assessed by agarose gel electrophoresis. The concentration of DNA was estimated at A_{260} nm and expressed as mol nucleotide residues/l.

Bacterial strains and media

Escherichia coli strain DH5α was used for plasmid manipulations and grown in liquid or solid LB agar supplemented with appropriate antibiotics. PI-MtuI was overproduced from pGRI in *E.coli* strain DH5α using iospropyl-1-thio-β-D-galactopyranoside and purified to homogeneity as described (13). The procedure used for purification of PI-MtuI mutants was identical (14). The identity of purified proteins was confirmed by Coomassie blue staining and western blot analysis using polyclonal antibodies raised against wild-type PI-MtuI (16). Protein concentrations were determined by the dye binding method using bovine serum albumin as standard (17). Protein preparations were found to be free of exonucleases as assessed by incubation with both single- and linear double-stranded M13 DNA.

Site-directed mutagenesis

Site-directed mutagenesis of the conserved amino acid residues was performed using an overlap extension PCR method (18). Briefly, single point mutations D122Y and D222T were generated using pEJ135 DNA as the template (14). PCR products were incubated with SmaI and AccI, separated by electrophoresis on an agarose gel and the DNA fragment (851 bp) was eluted from the gel (19). It was ligated into pGEX-2T, which had been digested with the same set of enzymes. After isolation of recombinant plasmid DNAs, mutants were identified by digestion with appropriate restriction endonucleases. The mutant constructs were verified by sequencing in an automated ABI Prism DNA sequencer (Perkin-Elmer Life Sciences). Recombinant plasmids were transformed and PI-MtuI variants were overproduced in *E.coli* strain DH5α. All PI-MtuI mutants showed similar levels of expression.

UV catalyzed crosslinking of ATP to PI-MtuI

Reaction mixtures (10 µl) contained 20 mM Tris–HCl buffer (pH 7.5), 0.4 mM dithiothreitol (DTT), 15 µM PI-MtuI and the indicated concentrations of [γ-^{32}P]ATP (6000 Ci/mmol). In competitive binding assays, after incubation of PI-MtuI with [γ-^{32}P]ATP for 5 min, unlabeled ATP was added to the reaction mixture at the indicated concentrations. Following incubation at 37°C for 5 min, samples were placed on ice at ~2 cm from the light source and subjected to irradiation at 254 nm for 5 min using a Hoefer Scientific crosslinker. Reaction mixtures were mixed with 2 µl of 5× SDS sample loading buffer (10 mM Tris–HCl, pH 6.8, 40% glycerol, 12.5% SDS and 25 mM DTT containing 0.1% bromophenol blue) and incubated at 94°C for 2 min. Samples were separated by 10% SDS–PAGE. The gel was washed extensively with methanol:acetic acid:water (10:10:80 v/v) solution to remove free ATP and dried over a Whatman 3MM filter at 80°C. The dried gel was exposed to a PhosphorImager screen for 3 h. Quantification of the bands corresponding to PI-MtuI was performed by Image Gauge ver. 3.0 (Fuji Science, Japan) and plotted using Graphpad Prism ver. 2.0. To determine the stoichiometry of binding of ATP to PI-MtuI, a fixed concentration of PI-MtuI (15 µM) was incubated with increasing concentrations of ATP. After UV crosslinking and autoradiography, the bands were quantified and plotted against increasing concentrations of ATP. The data was subjected to non-linear regression analysis and was found to fit a one site binding model derived using the equation $Y = B_{max} \times X/[K_d + X]$, where X and Y represent the amount of ATP and ATP crosslinked to PI-MtuI, respectively, B_{max} is the maximal binding of ATP and K_d is the concentration of ATP required to attain half-maximal binding.

ATPase assay

The ATPase assay was performed as described (20) with modifications. Briefly, reaction mixtures (10 µl) contained 25 mM Tris–HCl buffer (pH 7.5), 0.4 mM DTT, 16 µM pEJ244 form I DNA and 3 mM $MnCl_2$ or 5 mM $MgCl_2$, where specified. In addition to the indicated concentrations of ATP, 200 nCi of [α-^{32}P]ATP was added to all the reaction mixtures as a tracer. Reactions were initiated with the addition of 3 µM PI-MtuI. After incubation for the indicated time intervals at 37°C, reactions were terminated with the addition of EDTA to a final concentration of 15 mM and extracted with chloroform. Samples were centrifuged at 10 000 r.p.m. for 5 min. Three microliter aliquots of the supernatant were spotted on PEI–cellulose TLC sheet and developed in a solution containing 0.5 M LiCl, 1 M HCOOH and 1 mM EDTA, dried and subjected to autoradiography. The bands corresponding to ^{32}P-labeled ATP and ADP were quantified by the image analyzer software UVI-BandMap ver. 99 and plotted using Graphpad Prism ver. 2.0. The kinetic parameters (K_m and V_{max}) were determined from the Lineweaver–Burk plot (1/[S] versus 1/v) using the equation $1/v = 1/V_{max} + K_m/V_{max}[S]$, where v is the velocity of the reaction and [S] is the concentration of the substrate. The k_{cat} value was calculated using the equation $k_{cat} = V_{max}/[E]_t$, where $[E]_t$ is the total enzyme concentration and V_{max} is the maximal velocity of the reaction determined from the reciprocal plot.

Endonuclease assay

Endonuclease assays were performed as described (13). Reaction mixtures (25 µl) contained 25 mM Tris–HCl buffer (pH 7.5), 0.4 mM DTT, 3 mM $MnCl_2$, 1.5 mM ATP, 16 µM form I pEJ244 DNA and 1 µM PI-MtuI. After incubation at 37°C for different intervals of time, reactions were stopped by the addition of SDS to a final concentration of 0.1% and the samples were deproteinized by incubation with 0.2 mg/ml proteinase K for 15 min at 37°C. Three microliters of gel

loading buffer (20% glycerol containing 0.12% w/v each of bromophenol blue and xylene cyanol) was added to each sample and the samples were separated on a 0.8% agarose gel in 89 mM Tris–borate buffer (pH 8.3) containing 2 mM EDTA at 3 V/cm. The gel was stained with ethidium bromide (0.5 μg/ml) and DNA was visualized by UV illumination. Subsequently, DNA was transferred to Nylon N^+ membrane and visualized by Southern hybridization (21). The bands were quantified in a UVI-Tech gel documentation station using UVI-BandMap ver. 99 and plotted using Graphpad Prism ver. 2.0.

Limited proteolysis of PI-MtuI by chymotrypsin

The appropriate concentration of chymotrypsin required for limited proteolysis of PI-MtuI was determined from serial dilutions. A concentration of 4 μg/ml generated reproducible profiles in the assay buffer indicated below. Reaction mixtures (250 μl) contained 25 mM Tris–HCl buffer (pH 7.5), 0.4 mM DTT, 70 μg PI-MtuI and 1.5 mM ATP, 16 μM pEJ244 form I DNA and 3 mM $MnCl_2$, where specified. The reaction was initiated with the addition of 1 μg bovine chymotrypsin. After incubation at 37°C for the indicated time intervals, aliquots (25 μl) were taken and mixed with 5 μl of 5× SDS sample buffer (10 mM Tris–HCl, pH 6.8, 40% glycerol, 12.5% SDS, 25 mM DTT containing 0.1% bromophenol blue) and 0.2 mM phenylmethylsulfonyl fluoride. Samples were analyzed by 10% SDS–PAGE, followed by staining with Coomassie Brilliant Blue R-250. Similarly, limited proteolysis of UV crosslinked ATP–PI-MtuI complex was performed as described above. A band corresponding to a 14 kDa fragment crosslinked to ATP was excised from the SDS–PAGE gel and subjected to electrospray mass spectrometric analysis.

RESULTS

ATP binding properties of PI-MtuI

We have previously reported that PI-MtuI displays dual target specificity in response to alternative cofactors (13,14). While both ATP and Mn^{2+} were required for optimal cleavage of cognate DNA, Mg^{2+} alone was sufficient for cleavage of ectopic DNA sites. To investigate the possibility of whether PI-MtuI can bind ATP, it was incubated with [γ-^{32}P]ATP in the absence or presence of metal ion cofactors. Subsequently, reaction mixtures were exposed to UV radiation to stabilize the PI-MtuI–ATP complex (21), separated by SDS–PAGE and the bound ATP was detected by autoradiography.

Control experiments showed that *M.tuberculosis* RecA bound substantial amounts of ATP, while its cognate single-stranded binding protein (SSB) did not (Fig. 1, lanes 1 and 2). In the absence of metal ions, ATP was bound to a truncated form of PI-MtuI (Fig. 1, lane 3). The relationship of the truncated form to full-length PI-MtuI was confirmed by western blot analysis with polyclonal antibodies raised against PI-MtuI (data not shown). The extent of binding of ATP to PI-MtuI was dependent on the type of metal ion. While PI-MtuI bound ATP with lower affinity in the presence of Mg^{2+}, binding was substantially higher in the presence of Mn^{2+} (Fig. 1, compare lanes 4 and 5 to 6 and 7). Together, these results suggest that the metal ions alter the affinity of

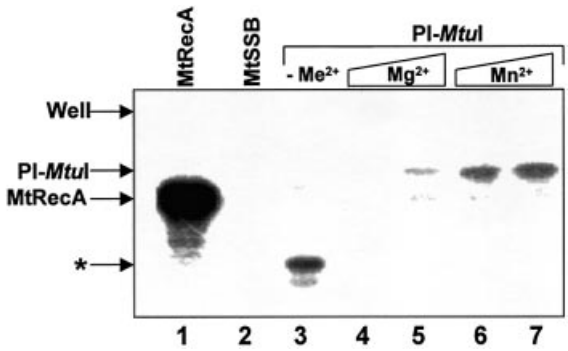

Figure 1. ATP binding to PI-MtuI as monitored by UV catalyzed crosslinking. Reactions were performed as described in Materials and Methods. The autoradiogram shows the SDS–PAGE analysis of photolabeled proteins. Lane 1, *M.tuberculosis* RecA protein (16 μM) in the presence of 2 mM $MgCl_2$ and 1.6 pmol [γ-^{32}P]ATP; lane 2, *M.tuberculosis* single-stranded DNA-binding protein (16 μM), 2 mM $MgCl_2$ and 1.6 pmol [γ-^{32}P]ATP; lane 3, PI-MtuI (16 μM) with 1.6 pmol [γ-^{32}P]ATP in the absence of added metal ion (–Me^{2+}). The remaining lanes contained PI-MtuI (16 μM) and the indicated cofactor(s): 2.5 mM $MgCl_2$ (lane 4), 5 mM $MgCl_2$ (lane 5), 2.5 mM $MnCl_2$ (lane 6); 5 mM $MnCl_2$ (lane 7). An asterisk denotes the truncated form of PI-MtuI.

PI-MtuI for ATP as well as confer protection against radiolysis.

Stoichiometric binding of ATP to PI-MtuI

To determine the stoichiometry of ATP-binding to PI-MtuI, a fixed concentration of PI-MtuI was incubated with increasing concentrations of [γ-^{32}P]ATP. The samples were incubated and assayed as described above. Figure 2A shows the extent of binding of ATP to PI-MtuI as a function of increasing amounts of ATP in the presence of Mn^{2+}. Quantification of the band intensity indicated that the amount of ATP bound to PI-MtuI was linear in the range 2.5–15 μM, above which the reaction progress curve deviated from linearity and displayed an apparent saturation effect (Fig. 2B). The binding data better fits a one-site binding hyperbolic curve with a half-maximal binding of 10 μM ATP. Although UV catalyzed crosslinking is not an equilibrium binding reaction, within its limits these results are consistent with binding of ~1 ATP/PI-MtuI monomer. To confirm the specificity of binding of ATP to PI-MtuI, we performed a competition binding assay as described in Materials and Methods. The results showed that PI-MtuI formed a stable complex with ATP, as a 10 000-fold excess of cold ATP was able to displace 80% of radiolabeled ATP (data not shown).

PI-MtuI is a (cognate) DNA-dependent ATPase

Previously, we showed that PI-MtuI exhibited pronounced dependence on ATP for cleavage of cognate DNA (13). Thus, we speculated that ATP hydrolysis might be crucial for its endonuclease activity. To investigate this directly, we performed ATPase assays in the presence of different cofactors. As shown in Figure 3, PI-MtuI by itself (lanes 2 and 9), or in the presence of DNA (lanes 4 and 11), was unable to catalyze ATP hydrolysis. On the other hand, in the presence of Mg^{2+} or together with cognate or ectopic DNA, PI-MtuI displayed residual activity (Fig. 3, lanes 3, 5 and 7). Also, PI-MtuI behaved qualitatively similarly in the presence of Mn^{2+} (Fig. 3,

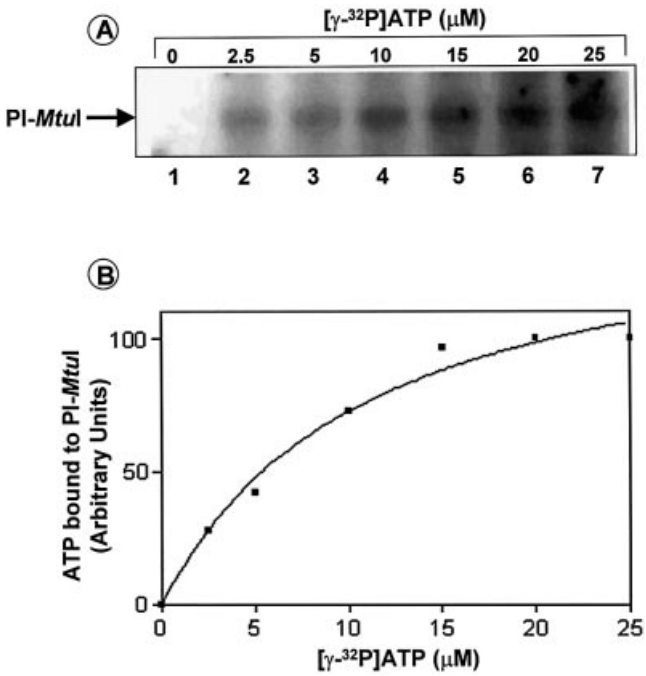

Figure 2. Binding of ^{32}P-labeled ATP to PI-MtuI as a function of ATP concentration. Reactions were performed with increasing concentrations of ATP as indicated above each lane. Reactions mixtures were analyzed as described in Materials and Methods. (**A**) Autoradiogram showing crosslinking of ATP to PI-MtuI. (**B**) Quantification of the extent of binding of labeled ATP. The intensity of bands was quantified after correcting the background using UVI-BandMap software ver. 99 and plotted against concentration of ATP using Graphpad Prism ver. 2.0. The graph shows the average of two independent experiments.

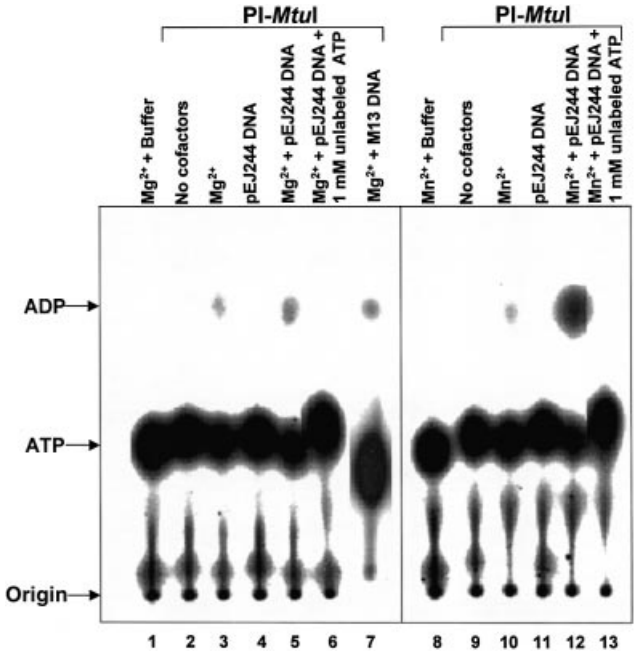

Figure 3. ATP hydrolysis catalyzed by PI-MtuI. Reactions were performed in the absence or presence of cofactors and/or DNA as described in Materials and Methods. An autoradiogram of a typical TLC analysis showing ADP generated during the reaction in the absence (lanes 2 and 9) or presence (lanes 1, 3–8 and 10–13) of different cofactors as indicated above each lane. The positions of ATP and ADP are shown on the left.

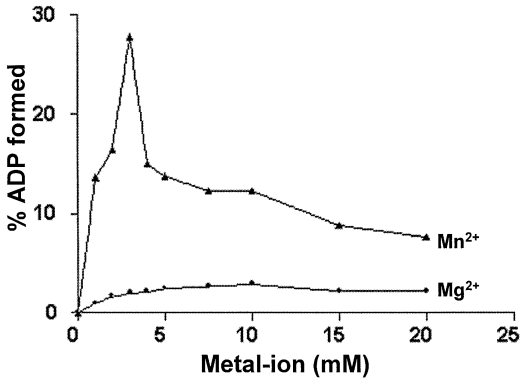

Figure 4. Effect of a metal ion on ATP hydrolysis catalyzed by PI-MtuI. ATPase assays were performed with increasing concentrations of Mg^{2+} or Mn^{2+}. Reactions were terminated and analyzed by TLC as described in Materials and Methods. The bands were quantified and plotted as a function of Mg^{2+} or Mn^{2+} concentration. ATP hydrolysis is expressed as a percentage of ADP formed from [α-^{32}P]ATP with respect to the value obtained in the absence of metal ions. The graph shows the average of two independent experiments.

lane 10). However, addition of cognate DNA led to a sharp increase in ATPase activity by 40-fold (Fig. 3, lane 12). The specificity of ATPase activity was confirmed by performing the reaction in the presence of cold ATP: addition of 1 mM ATP completely abolished ATP hydrolysis (Fig. 3, lanes 6 and 13). Under these conditions, ectopic DNA failed to stimulate ATPase activity in the presence of Mg^{2+} (Fig. 3, lane 7, and see below). Together, these data suggest that PI-MtuI is a Mn^{2+}- and (cognate) DNA-dependent ATPase.

To further characterize ATP hydrolysis catalyzed by PI-MtuI, reactions were performed in the presence of cognate DNA with increasing concentrations of either Mg^{2+} or Mn^{2+}. As shown in Figure 4, the formation of ADP was measurable but remained constant across the indicated concentrations of Mg^{2+}. In contrast, accumulation of ADP increased sharply with increasing concentrations of Mn^{2+}, reaching a maximum at 3 mM and decreasing sharply thereafter. This concentration of Mn^{2+} is quantitatively similar to the amount required for the display of its optimal endonuclease activity (13).

In subsequent experiments, we analyzed the kinetics of ATP hydrolysis in the absence or presence of either cognate or ectopic DNA. In the absence of DNA, formation of ADP was measurable but remained lower throughout the incubation period (Fig. 5, closed triangles). On the other hand, PI-MtuI was able to catalyze ATP hydrolysis in the presence of both cognate and ectopic DNA. However, greater stimulation was observed with Mn^{2+} and cognate DNA compared to ectopic DNA and Mg^{2+} (Fig. 5, compare closed squares to inverted closed triangles). In the presence of Mn^{2+} and cognate DNA, PI-MtuI displayed a striking increase in the extent of formation of ADP up to 40 min, above which it reached a plateau. The basis for the differences in amplitudes seen between cognate DNA and Mn^{2+} versus ectopic DNA and Mg^{2+} remains to be investigated.

Kinetic analysis of ATP hydrolysis catalyzed by PI-MtuI

The effect of increasing ATP concentration on the PI-MtuI catalyzed reaction was investigated by kinetic experiments.

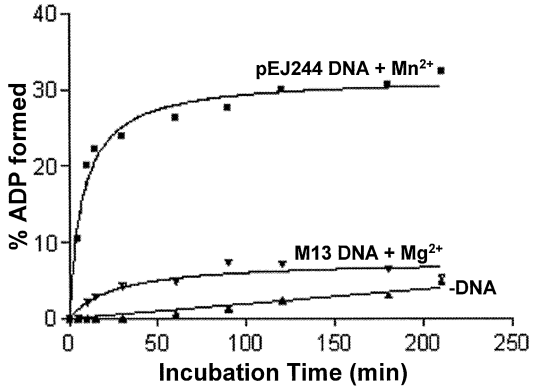

Figure 5. PI-MtuI is a Mn^{2+}- and (cognate) DNA-dependent ATPase. ATP hydrolysis was performed in an assay buffer containing PI-MtuI (3 μM) and cognate or ectopic DNA (16 μM) in the presence of either 3 mM Mn^{2+} or Mg^{2+} as described in Materials and Methods. The bands corresponding to ADP in the autoradiogram were quantified and plotted against time of incubation using Graphpad Prism ver. 2.0. The graph shows the mean of three independent experiments.

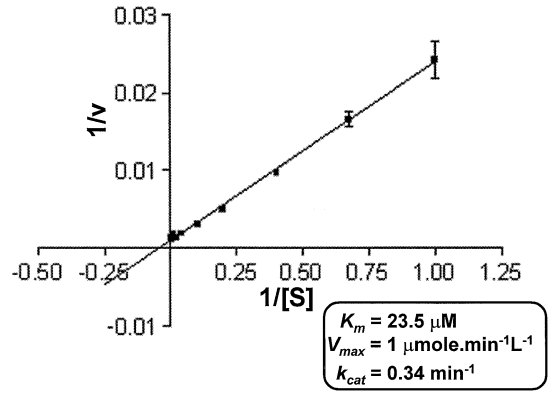

Figure 6. ATP hydrolysis catalyzed by PI-MtuI follows Michaelis–Menten kinetics. Reactions were performed at different concentrations of the substrate with a fixed concentration of PI-MtuI in the presence of 3 mM Mn^{2+}. Reaction products were separated by TLC and visualized by autoradiography. Quantification was performed as described in Materials and Methods. The rate of the reaction was calculated from the slopes of such plots. The figure shows $1/v$ versus $1/[S]$ in the form of a Lineweaver–Burk plot. The inset shows the summary of kinetic parameters for wild-type PI-MtuI. The graph shows the mean ± SD of three independent experiments.

The reactions were performed with a fixed concentration of PI-MtuI, Mn^{2+} and cognate DNA, but at varying concentrations of ATP. The velocities were determined from the linear phase of the reaction progress curve across a range of ATP concentrations from 0.25 to 100 μM. A plot representing rates of ATP hydrolysis versus substrate concentration revealed a hyperbolic character, indicating typical Michaelis–Menten kinetics. The data from the linear phase of the curve was fitted to a Lineweaver–Burk plot (Fig. 6). With cognate DNA as the substrate, we determined the empirical kinetic parameters for PI-MtuI. It has a $K_{m\ [ATP]}$ of 23.52 μM, k_{cat} of 0.34 per min and V_{max} of 1 μmol/min/l. Although PI-MtuI displayed a high affinity for ATP, the turnover number (k_{cat} = 0.34 per min) is lower. The low k_{cat}/K_m value suggests that a weak ATPase activity of PI-MtuI might account for inefficient cleavage of cognate DNA (13; this study). In comparison, the k_{cat} of PI-MtuI is 3.4-fold higher than Rad51 protein, but 29- and 65-fold weaker than *M.tuberculosis* and *E.coli* RecA proteins, respectively (22–26).

PI-MtuI variants display decreased ability to bind ATP

Previously, we had noticed that mutation of metal ion-binding acidic amino acids in the LAGLIDADG motifs of PI-MtuI led to abolition of cognate DNA cleavage (13). To explore the basis for loss of endonuclease activity, as a first step we wished to determine binding of ATP to PI-MtuI variants by UV catalyzed crosslinking. For this purpose, PI-MtuI variants were purified to homogeneity. The results of CD measurements revealed that the overall features of mutant enzyme structures were similar to that of wild-type PI-MtuI (data not shown). The UV crosslinking results showed that the amount of ATP bound by wild-type PI-MtuI was quantitatively similar to that noted above (Fig. 2). In comparison, the D122Y and D222T variants showed reduced ATP binding (Fig. 7A and B). Corroborating this observation, the kinetics of ATP hydrolysis revealed that D222T was totally inactive, while D122Y showed a substantial reduction in ATPase activity (Fig. 7C). Interestingly, the difference in ATP binding between the wild-type and variants of PI-MtuI is less substantial than the reduction in ATPase activity.

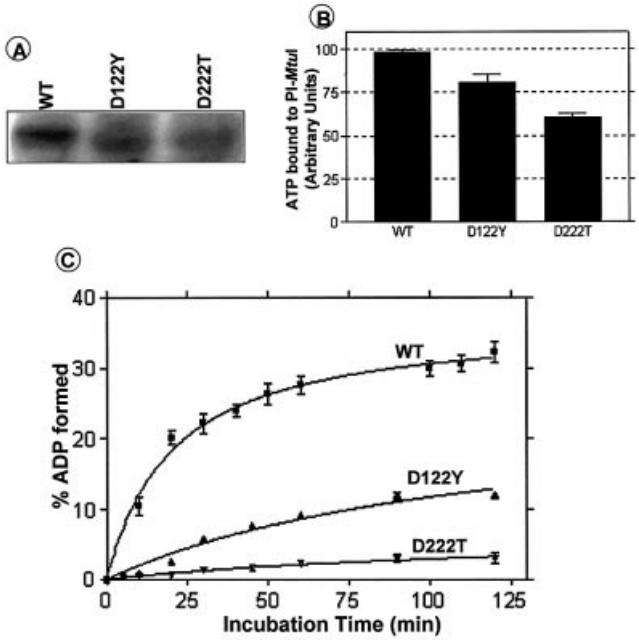

Figure 7. Mutation of conserved amino acid residues in the LAGLIDADG motifs of PI-MtuI affect binding of ATP and its hydrolysis. (**A**) Autoradiogram showing the binding of ATP by wild-type and variants of PI-MtuI. (**B**) Quantification of the extent of binding of ATP by wild-type and variants of PI-MtuI shown in (A). (**C**) Kinetics of ATPase activity of wild-type and variants of PI-MtuI. The ATPase assay was performed as described in Materials and Methods. The graph shows the mean ± SD of three independent experiments.

Correlation between ATPase and endonuclease activities

The above results raised the possibility that the ATPase activity of PI-MtuI might be crucial for its endonuclease

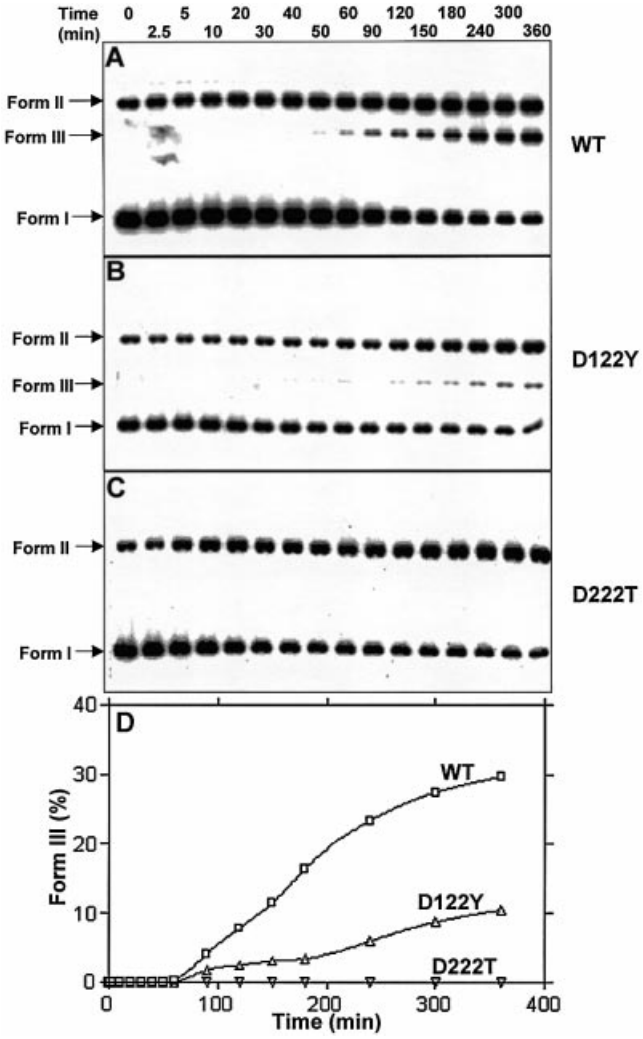

Figure 8. Kinetics of cognate DNA cleavage by wild-type and variants of PI-MtuI. Reactions containing wild-type (**A**) or variants (**B** and **C**) of PI-MtuI were performed as described in Materials and Methods. (**D**) Quantification of the extent of cognate DNA cleavage by wild-type and variants of PI-MtuI shown in (A–C). The graph shows the mean of two independent experiments. Form I, negatively supercoiled DNA; Form II, nicked circular DNA; Form III, linear double-stranded DNA.

function. To address this question directly, we compared the endonuclease activity of wild-type and variants of PI-MtuI using cognate DNA as the substrate. In contrast to the wild-type, D122Y, which showed residual ATPase activity, displayed weak endonuclease function (compare Fig. 8A to B). A similar observation had previously been made with D122Y while studying its DNA cleavage specificity in the presence of alternative metal ion cofactors (14). Further studies of the cleavage reaction highlighted that while D222T failed to cleave sequence spanning the homing site, D122Y exhibited an altered cleavage specificity (data not shown). Importantly, the D222T variant, which was unable to catalyze ATP hydrolysis, failed to generate form III DNA (Fig. 8C). However, both mutants were able to convert a significant amount of form I DNA to form II DNA. Indeed, a reduction in or loss of ATPase activity of PI-MtuI was correlated with its endonuclease activity (Fig. 8D).

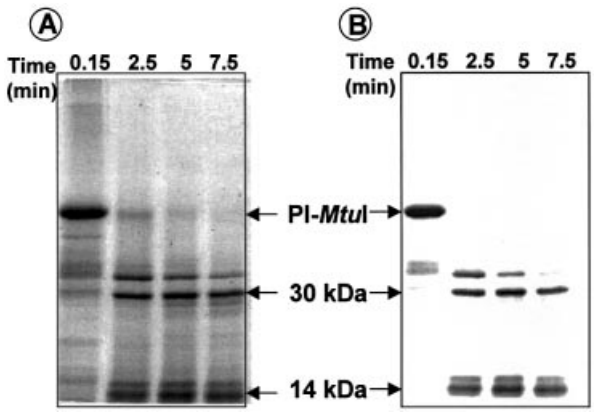

Figure 9. Isolation of 14 kDa peptide. PI-MtuI was crosslinked to [γ-^{32}P]ATP and subjected to limited proteolysis with chymotrypsin as described in Materials and Methods. (**A**) Coomassie blue stained SDS–PAGE gel showing the partial chymotryptic digest. (**B**) Autoradiogram of the gel shown in (A).

Sequence analysis of the photolabeled truncated derivative of PI-MtuI

Since the atomic structure of PI-MtuI is not yet available, identification of its ATP-binding domain might help uncover its mechanism of action. To identify the ATP-binding motif, ^{32}P-labeled ATP was crosslinked to PI-MtuI and subjected to limited proteolysis by chymotrypsin (Fig. 9A), and the reaction mixtures were analyzed as described in Materials and Methods. As shown in Figure 9B, ^{32}P-labeled ATP was found to be associated with a 14 kDa peptide. This band was excised from the gel and separated by SDS–PAGE. The radioactive peptide was in-gel trypsinized, eluted and subjected to electrospray ionization mass spectrometric analysis. The results suggested that the 14 kDa fragment comprising amino acids 8–132 in full-length PI-MtuI contained the putative ATP-binding motif (^{125}GxxGGKT^{131}).

Cofactors induce structural transitions in PI-MtuI

The limited proteolysis approach has been widely used as a sensitive tool to monitor structural transitions in proteins associated with specific binding of ligands (27). Accordingly, first we treated PI-MtuI with a limiting concentration of chymotrypsin in the presence of buffer alone. At specified time intervals, the reaction was terminated and samples were separated by SDS–PAGE, and the gel was visualized by staining with Coomassie blue. In the absence of cofactors, >80% of full-length PI-MtuI was cleaved by 30 min, generating three prominent fragments of 30, 14 and 10 kDa (denoted by asterisks in Fig. 10A). Mapping of the cleavage sites and location of these fragments within PI-MtuI is currently under investigation. A caveat is that the differences in the cleavage pattern could arise from differential activity of chymotrypsin in response to the indicated metal ions. This possibility seemed unlikely, since similar cleavage profiles were observed in the presence of trypsin (data not shown).

Because both Mn^{2+} and ATP were required for cleavage of cognate DNA by PI-MtuI, it seemed likely that they might induce structural changes in full-length PI-MtuI. However, the results shown in Figure 10B suggest that the extent of cleavage

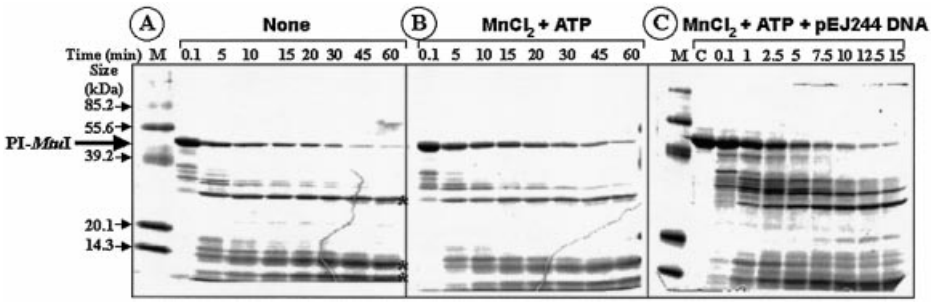

Figure 10. The effect of cofactors and DNA on limited proteolysis of PI-MtuI. Products of the proteolysis reaction in the absence of cofactors (**A**) or in the presence of 3 mM Mn^{2+} and 1.5 mM ATP (**B**) or cognate DNA (16 µM), 3 mM Mn^{2+} and 1.5 mM ATP (**C**). In each lane, ~7 µg of PI-MtuI incubated with 1 µl of 0.1 mg/ml bovine chymotrypsin for the indicated time interval was loaded as described in Materials and Methods. The time of digestion (min) is indicated at the top of each panel. The reaction was terminated by the addition of 5 µl of 5× SDS loading buffer. Samples were separated by 10% SDS–PAGE and visualized by staining with Coomassie blue. Lane M, molecular mass markers (Combithek; Boehringer Mannheim Biochemica), with size in kDa indicated on the left. Asterisks represent the major proteolysis fragments of PI-MtuI.

of full-length PI-MtuI in the presence of Mn^{2+} and ATP was largely similar to the results obtained with PI-MtuI alone (compare Fig. 10A to B). To investigate the effect of DNA, we incubated PI-MtuI with ATP and Mn^{2+} in the presence of cognate DNA. The samples were then treated with chymotrypsin and analyzed as described in Materials and Methods. Interestingly, addition of DNA led to robust and rapid cleavage: >90% of full-length PI-MtuI was digested within 10 min, indicating that DNA uncovers chymotrypsin-accessible sites in PI-MtuI (compare Fig. 10B to C). These results suggest that cleavage sites that are less accessible in the absence or presence of cofactors become more exposed upon interaction with DNA.

DISCUSSION

In this study, we show that the RecA intein, a LAGLIDADG homing endonuclease, is a (cognate) DNA- and Mn^{2+}-dependent ATPase. Several controls and observations indicate that the intrinsic ATPase activity of PI-MtuI is crucial for its endonuclease function. First, a single peak of ATPase activity co-eluted with PI-MtuI during chromatography (data not shown). Second, PI-MtuI by itself was unable to catalyze ATP hydrolysis. Importantly, cognate DNA stimulated PI-MtuI to hydrolyze ATP much more efficiently compared to ectopic DNA sites. Third, the extent of stimulation of ATPase activity by Mn^{2+} was greater than Mg^{2+}. Finally, a PI-MtuI variant that showed loss of ATPase activity was inactive in DNA cleavage, emphasizing the notion that ATPase activity is crucial for its endonuclease function.

It is intriguing that PI-MtuI required ATP binding as well as its hydrolysis for the display of its endonuclease activity with cognate DNA, a property different from other known LAGLIDADG homing endonucleases. Why might PI-MtuI require ATP hydrolysis for its endonuclease function? One possible role would be that ATP hydrolysis is required for turnover of the enzyme. Alternatively, or in addition, ATP hydrolysis may be required for its processive tracking along DNA and for distortion of its cleavage sequence. Thus, the D222T mutation, which resulted in total loss of ATPase activity, concomitantly abolished endonuclease function. On the other hand, the D122Y variant, which hydrolyzes ATP poorly, displayed weak endonuclease activity. The molecular defect responsible for reduced ATP binding by the D122Y and D222T variants is likely due to weakened interaction of PI-MtuI with ATP·Mn^{2+} complex. In addition, our results show that Mn^{2+} plays a dual role in PI-MtuI function: it is essential for ATPase as well as endonuclease activities. We note that maximum stimulation of ATPase activity was achieved in the presence of cognate DNA, but not ectopic DNA. An interesting analogy is found in the case of *M.tuberculosis* RecA, which is also generated by splicing of the RecA precursor. However, RecA differs from PI-MtuI in that its ATPase activity is greater in the presence of single-stranded DNA and Mg^{2+}. That Mg^{2+} was unable to support ATP hydrolysis by PI-MtuI with cognate DNA is surprising, since many DNA-dependent ATPases prefer Mg^{2+} as the metal ion cofactor (28).

Sequence analysis revealed that PI-MtuI harbors two copies of the LAGLIDADG motif. The sequence of the first motif is ^{115}LLGYLIGD*G^{123} and of the second ^{214}LLFGLFE*SD*G^{223} (asterisks denote conserved acidic amino acids). It remains to be elucidated whether binding of Mn^{2+} as well as Mg^{2+} involves the same LAGLIDADG motif or both in the PI-MtuI monomer. Analysis of the PI-MtuI D122Y and D222T variants suggested that both Mn^{2+} and Mg^{2+} might interact with the same LAGLIDADG motif (14). We believe that firm evidence for involvement of the LAGLIDADG motif in binding of metal ions must come from the crystal structure. This is important because, on the basis of mutational analysis of I-PpoI homing endonuclease, it was inferred that the PD^{109}xxxxD^{140}NK motif is the Mg^{2+}-binding site. However, this was not evident in the co-crystal structure of I-PpoI (29,30). Thus far, PI-MtuI is the only LAGLIDADG homing endonuclease known to require ATP hydrolysis for cleavage of cognate DNA. Consistent with this, previously we showed that ATPγS failed to support cleavage of cognate DNA (13).

Several lines of evidence suggest that binding of ligands induces distinct structural alterations in proteins (31,32). Indeed, PI-SceI undergoes substantial structural changes upon binding to DNA (33). Similarly, limited proteolysis experiments revealed substantial conformational rearrangements in PI-MtuI during binding of DNA and its cleavage. Likewise, a cofactor-induced extended conformational state has been presumed to represent the catalytically active form of I-TevI

(34). In conclusion, our results have revealed dynamic interactions between PI-MtuI and cognate DNA as well as cofactors. Furthermore, hydrolysis of ATP catalyzed by PI-MtuI in the context of Mn^{2+} and (cognate) DNA is intrinsically coupled to its endonuclease activity. In this regard, PI-MtuI is fundamentally unique among the members of the LAGLIDADG superfamily of homing endonucleases.

ACKNOWLEDGEMENTS

ESI-mass spectrometric analysis was carried out at the Laboratory for Proteomic Mass Spectrometry, University of Massachusetts Medical School. This work was supported by grants from the Wellcome Trust, UK and Indian Council of Medical Research, New Delhi, India. N.G. was supported by a fellowship from the Council of Scientific and Industrial Research, New Delhi, India.

REFERENCES

1. Belfort,M. and Roberts,R.J. (1997) Homing endonucleases: keeping the house in order. *Nucleic Acids Res.*, **25**, 3379–3388.
2. Liu,X.Q. (2000) Protein-splicing intein: genetic mobility, origin and evolution. *Annu. Rev. Genet.*, **34**, 61–76.
3. Noren,C.J., Wang,J. and Perler,F.B. (2000) Dissecting the chemistry of protein splicing and its applications. *Angew. Chem. Int. Ed. Engl.*, **39**, 450–466.
4. Gimble,F.S. (2000) Invasion of a multitude of genetic niches by mobile endonuclease genes. *FEMS Microbiol. Lett.*, **185**, 99–107.
5. Jurica,M.S. and Stoddard,B.L. (1999) Homing endonucleases: structure, function and evolution. *Cell. Mol. Life Sci.*, **55**, 1304–1326.
6. Chevalier,B.S. and Stoddard,B.L. (2001) Homing endonucleases: structural and functional insight into the catalysis of intron/intein mobility. *Nucleic Acids Res.*, **29**, 3757–3774.
7. Mueller,J.E., Bryk,M., Loizos,N. and Belfort,M. (1993) Homing endonucleases. In Linn,S.M., Lloyd,R.S. and Roberts,R.J. (eds), *Nucleases*. Cold Spring Harbor Laboratory Press, Cold Spring Harbor, NY, pp. 111–144.
8. Lambowitz,A.M. and Belfort,M. (1993) Introns as mobile genetic elements. *Annu. Rev. Biochem.*, **62**, 587–622.
9. Wang,J., Kim,H.H., Yuan,X. and Herrin,D.L. (1997) Purification, biochemical characterization and protein–DNA interactions of the I-*Cre*I endonuclease produced in *Escherichia coli*. *Nucleic Acids Res.*, **25**, 3767–3776.
10. Jurica,M.S., Monnat,R.J.,Jr and Stoddard,B.L. (1998) DNA recognition and cleavage by the LAGLIDADG homing endonuclease I-*Cre*I. *Mol. Cell*, **2**, 469–476.
11. Dalgaard,J.Z., Garrett,R.A. and Belfort,M. (1994) Purification and characterization of two forms of I-*Dmo*I, a thermophilic site-specific endonuclease encoded by an archaeal intron. *J. Biol. Chem.*, **269**, 28885–28892.
12. Christ,F., Schoettler,S., Wende,W., Steuer,S., Pingoud,A. and Pingoud,V. (1999) The monomeric homing endonuclease PI-*Sce*I has two catalytic centres for cleavage of the two strands of its DNA substrate. *EMBO J.*, **18**, 6908–6916.
13. Guhan,N. and Muniyappa,K. (2002) *Mycobacterium tuberculosis* RecA intein possesses a novel ATP-dependent site-specific double-stranded DNA endonuclease activity. *J. Biol. Chem.*, **277**, 16257–16264.
14. Guhan,N. and Muniyappa, K (2002) The RecA intein of *Mycobacterium tuberculosis* promotes cleavage of ectopic DNA sites: implications for the dispersal of inteins in natural populations *J. Biol. Chem.*, **277**, 40352–40361.
15. Cunningham,R.P., DasGupta,C., Shibata,T. and Radding,C.M. (1980) Homologous pairing in genetic recombination: recA protein makes joint molecules of gapped circular DNA and closed circular DNA. *Cell*, **20**, 223–235.
16. Bakshi,R.P., Galande,S., Bali,P., Dighe,R. and Muniyappa,K. (2001) Developmental and hormonal regulation of type II DNA topoisomerase in rat testis. *J. Mol. Endocrinol.*, **26**, 193–206.
17. Bradford,M.M. (1976) A rapid and sensitive method for the quantitation of microgram quantities of protein utilizing the principle of protein-dye binding. *Anal. Biochem.*, **72**, 248–254.
18. Aiyar,A., Xiang,Y. and Leis,J. (1996) Site-directed mutagenesis using overlap extension PCR. *Methods Mol. Biol.*, **57**, 177–191.
19. Sambrook,J., Fritsch,E.F. and Maniatis,T. (1989) *Molecular Cloning: A Laboratory Manual*, 2nd Edn. Cold Spring Harbor Laboratory Press, Cold Spring Harbor, NY.
20. Shibata,T., Cunningham,R.P. and Radding,C.M. (1981) Homologous pairing in genetic recombination. Purification and characterization of *Escherichia coli* recA protein. *J. Biol. Chem.*, **256**, 7557–7564.
21. Meffert,R., Dose,K., Rathgeber,G. and Schafer,H.J. (2001) Ultraviolet crosslinking of DNA-protein complexes via 8-azidoadenine. *Methods Mol. Biol.*, **148**, 323–335.
22. Tombline,G. and Fishel,R. (2002) Biochemical characterization of the human RAD51 protein. I. ATP hydrolysis. *J. Biol. Chem.*, **277**, 14417–14425.
23. Baumann,P., Benson,F.E. and West,S.C. (1996) Human Rad51 protein promotes ATP-dependent homologous pairing and strand transfer reactions *in vitro*. *Cell*, **87**, 757–766.
24. Schutte,B.C. and Cox,M.M. (1987) Homology-dependent changes in adenosine 5′-triphosphate hydrolysis during recA protein promoted DNA strand exchange: evidence for long paranemic complexes. *Biochemistry*, **26**, 5616–5625.
25. Menetski,J., Varghese,A. and Kowalczykowski,S.C. (1988) Properties of the high-affinity single-stranded DNA binding state of the *Escherichia coli* recA protein. *Biochemistry*, **27**, 1205–1212.
26. Kumar,R.A., Vaze,M.B., Chandra,N.R., Vijayan,M. and Muniyappa,K. (1996) Functional characterization of the precursor and spliced forms of RecA protein of *Mycobacterium tuberculosis*. *Biochemistry*, **35**, 1793–1802.
27. Trapp,T. and Holsboer,F. (1995) Ligand-induced changes in the mineralocorticoid receptor analyzed by protease mapping. *Biochem. Biophys. Res. Commun.*, **215**, 286–291.
28. Cowan,J.A. (1998) Metal activation of enzymes in nucleic acid biochemistry. *Chem. Rev.*, **98**, 1067–1087.
29. Wittmayer,P.K. and Raines,R.T. (1996) Substrate binding and turnover by the highly specific I-*Ppo*I endonuclease. *Biochemistry*, **35**, 1076–1083.
30. Flick,K.E., Jurica,M.S., Monnat,R.J.,Jr and Stoddard,B.L. (1998) DNA binding and cleavage by the nuclear intron-encoded homing endonuclease I-*Ppo*I. *Nature*, **394**, 96–101.
31. Newman,M., Strzelecka,T., Dorner,L.F., Schildkraut,I. and Aggarwal,A.K. (1995) Structure of *Bam*HI endonuclease bound to DNA: partial folding and unfolding on DNA binding. *Science*, **269**, 656–663.
32. Winkler,F.K., Banner,D.W., Oefner,C., Tsernoglou,D., Brown,R.S., Heathman,S.P., Bryan,R.K., Martin,P.D., Petratos,K. and Wilson,K.S. (1993) The crystal structure of *Eco*RV endonuclease and its complexes with cognate and non-cognate DNA fragments. *EMBO J.*, **12**, 1781–1795.
33. Moure,C.M., Gimble,F.S. and Quiocho,F.A. (2002) Crystal structure of the intein homing endonuclease PI-*Sce*I bound to its recognition sequence. *Nature Struct. Biol.*, **9**, 764–770.
34. VanRoey,P., Wadding,C.A., Fox,K.M., Belfort,M. and Derbyshire,V. (2001) Intertwined structure of the DNA-binding domain of intron endonuclease I-*Tev*I with its substrate. *EMBO J.*, **20**, 3631–3637.